Thermoelectric and bulk mobility measurements in pentacene thin films

G.-H. Kim, M. Shtein, and K. P. Pipe

Citation: Applied Physics Letters **98**, 093303 (2011); doi: 10.1063/1.3556622

View online: http://dx.doi.org/10.1063/1.3556622

View Table of Contents: http://scitation.aip.org/content/aip/journal/apl/98/9?ver=pdfcov

Published by the AIP Publishing

Thermoelectric and bulk mobility measurements in pentacene thin films

G.-H. Kim,[1] M. Shtein,[2,a)] and K. P. Pipe[1,b)]
[1]*Department of Mechanical Engineering, University of Michigan, Ann Arbor, Michigan 48109, USA*
[2]*Department of Materials Science and Engineering, University of Michigan, Ann Arbor, Michigan 48109, USA*

(Received 19 October 2010; accepted 24 January 2011; published online 2 March 2011)

Low-noise thermoelectric and electrical measurements were used to derive the dependences of Seebeck coefficient and hole mobility on carrier concentration and grain size in the "bulk" regions of thermally evaporated pentacene thin films (in contrast to the channel field-effect mobility typically measured using thin-film transistor geometries). Distinct charge transport regimes were observed for larger (0.5 and 0.8 μm) and smaller (0.2 μm) grain sizes, attributed to carrier-dopant scattering and percolation, respectively. © *2011 American Institute of Physics*.
[doi:10.1063/1.3556622]

Organic semiconductors have demonstrated promise for a number of electronic[1,2] and optoelectronic[3,4] device applications, and recently have been investigated for potential use in thermoelectric energy conversion.[5–7] For this latter application, conversion efficiency is dictated by the thermoelectric figure-of-merit $Z=S^2\sigma/\kappa$, where S is the Seebeck coefficient and σ and κ are the electrical and thermal conductivities, respectively. Organic semiconducting materials offer low thermal conductivity as well as low cost, light weight, mechanical flexibility, capability for large-area deposition, yet their low thermoelectric power factor ($S^2\sigma$) has so far precluded their use in thermoelectric devices. However, the large existing library of organic compounds as well as the many ways in which these compounds may be functionalized to tune electrical (and thermal) properties offers numerous possible routes to optimize thermoelectric properties that are as yet unexplored.

While previous studies have measured the thermoelectric properties of inverted channels in organic thin film transistors,[8,9] very few studies have examined the bulk thermoelectric properties of organic thin films,[10,11] which are more relevant for thermoelectric device applications. Because the bulk electrical resistance of organic thin films is typically quite high, measurements of induced thermal voltage can have a poor signal-to-noise ratio, leading to difficult interpretation of measured results. Here, we demonstrate low-noise measurement of the Seebeck coefficient and electrical conductivity of pentacene thin films, assessing the dependence of these parameters on carrier density and grain size. Because the Seebeck coefficient is primarily a function of carrier density, we use it to derive the bulk mobility of these films as a function of the aforementioned properties, showing distinct transport regimes for different grain sizes.

Samples consisted of 60 nm thick pentacene (Lumtech Corp., 99% purity) thermally evaporated at 10^{-7} Torr onto solvent-cleaned, 1 mm thick glass slides at rates in the range of 0.4 Å/s to 0.04 Å/s, yielding a range of grain sizes that were characterized by atomic force microscopy. 50 nm of gold was deposited onto the pentacene through a shadow mask at a rate of 0.1 Å/s to define 1 mm wide $\times 5$ mm long contacts. Contacts were positioned in rows, with each row having a pair of contacts in which the short ends were separated by a gap length d of 25, 50, or 75 μm. The samples were then doped by exposure to iodine (Aldrich, 99.99% purity) for 1 h at room temperature to yield a saturated iodine concentration in the film.[12] Measurements of electrical conductivity and Seebeck coefficient were performed in atmosphere, while iodine evaporated from the film providing data on these parameters over a range of carrier concentrations.

The temperature gradients used to induce thermoelectric voltage were applied by a Peltier cooler (300 K$-\Delta T_0$) and Peltier heater (300 K$+\Delta T_0$) situated next to each other between the sample and a liquid-cooled heat sink. Two microthermocouples (TCs) of 25 μm diameter and 10 mK resolution were brought into contact with the gold electrodes under a microscope using micromanipulators. The distance between the TCs was set at 2 mm (measured with an error less than 2% using a reticle), which is much larger than the TC diameter, the gap length (d), and the error in TC position. Because the measured ΔT_{TC} and inter-TC distance (L) were much larger than their errors, the error in the derived temperature gradient ($\Delta T_{TC}/L$) was small. This temperature gradient was used to calculate the temperature difference across the gap (shown in Fig. 1) as $\Delta T=d\times\Delta T_{TC}/L$. Calculations of $\Delta T_{TC}/L$ were performed at different TC spacings ($L=1$, 2, 3, 4, and 5 mm), both on and off of the electrodes, and also on bare glass slides with no pentacene, without observing a significant change in $\Delta T_{TC}/L$. This implies that the temperature gradient was governed by the glass slide and was nearly

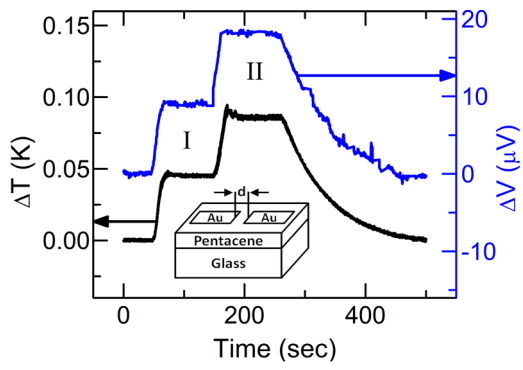

FIG. 1. (Color online) Applied temperature difference and induced thermal voltage measured between two electrodes as a function of time, for a pentacene sample with 0.8 μm grain size. The particular measurements shown in this figure were taken consecutively rather than simultaneously.

a)Electronic mail: mshtein@umich.edu.
b)Electronic mail: pipe@umich.edu.

independent of the presence of the pentacene thin film or the gold electrodes.

To measure thermal voltage, two thin gold wires of 50 μm diameter were brought into contact with the gold electrodes 1 mm apart under a microscope using micromanipulators, and were attached to bulk voltage probes whose temperature was maintained at a constant 300 K. Because the temperature gradient was controlled so that the temperature at the midpoint of the gap was 300 K, any parasitic thermal voltage in the gold electrodes was cancelled out by the thermal voltage in the gold wires. This was confirmed in a separate measurement in which the gold wires were brought into contact 1 mm apart on the same electrode and zero thermal voltage was measured. The measured thermal voltage was, therefore, only composed of the thermal voltage of the pentacene in the gap and was independent of the placement of the gold wires on the electrodes. Three gap widths (25, 50, and 75 μm) were tested in order to assess any parasitic effects that might arise at the contacts between the gold electrodes and the pentacene film. The measured thermal voltages increased proportional to the gap width, implying that no such parasitic effects were significant.

Electrical resistance was determined from a linear fit to the I-V curve measured by a semiconductor parameter analyzer (HP 4156B) and was in the range of 0.1 to 50 MΩ during dedoping for various grain sizes. To measure the induced thermal voltage at resistances in this high range, an instrumentation amplifier circuit with an input bias current less than 50 fA was built. Electrical and thermal measurement probes were electrically isolated from each other to minimize rf noise. The measured I-V curves showed good Ohmic behavior, consistent with the lack of parasitic thermal voltage effects observed at the contacts as discussed above.

During the first measurement sequence ("I" in Fig. 1), a temperature gradient was applied, and thermocouple readings were observed until the temperatures stabilized (this typically took 30 s). After these temperatures were recorded, thermal voltage measurements were recorded at a rate of 2 Hz and averaged over a certain time period, after which the I-V curve was measured to determine the electrical conductivity. A larger temperature gradient was then applied, and the same sequence was repeated ("II" in Fig. 1). Afterwards, the Peltier cooler and heater were turned off, and the thermal voltage was monitored until it returned to zero and the next I/II measurement pair was performed. The cycle was repeated until the drop in carrier concentration due to dedoping caused the resistance to increase beyond the highest measurable value (~50 MΩ). The time period of thermal voltage measurements was typically 100 s but was reduced somewhat for the highest carrier concentrations, which exhibited the fastest dedoping as measured by the I-V curves. The time period between I/II measurement pairs was typically 300 s, but was extended somewhat for the lowest carrier concentrations, which exhibited the slowest dedoping rate. Measured electrical conductivities were found to change only slightly within each I/II measurement pair, allowing an accurate determination of the Seebeck coefficient ($S=\Delta V/\Delta T$) as a function of carrier concentration by averaging the electrical conductivity, thermal voltage (ΔV), and temperature gradient (ΔT) for each I/II measurement pair. We note that the example data shown in Fig. 1 was taken in consecutive rather than simultaneous measurements and is included primarily to illustrate the low noise level of the thermal voltage and temperature measurements. Increased noise precluded the simultaneous collection of thermal voltage and temperature data by a computer running LABVIEW; during actual measurements, temperature data was observed and stabilized values recorded manually as discussed above.

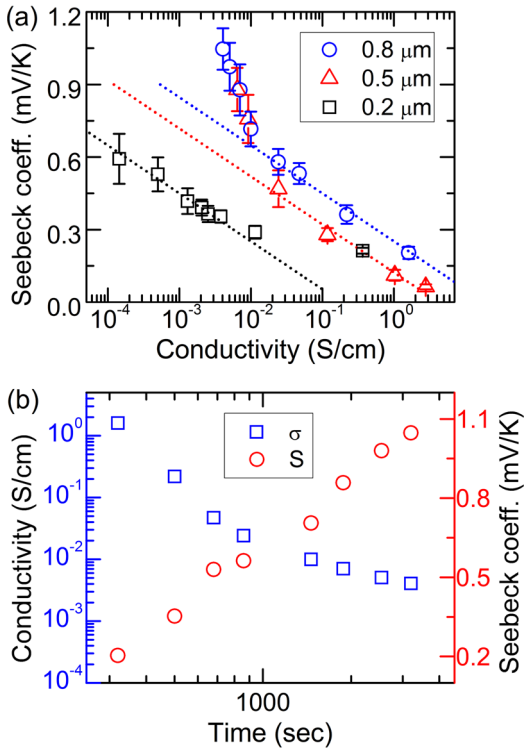

FIG. 2. (Color online) (a) Measured Seebeck coefficient plotted as a function of conductivity for 3 pentacene samples having 0.2, 0.5, and 0.8 μm grain sizes, where the dotted lines correspond to a slope of $-k/q$ as expressed in Eq. (3), and (b) measured Seebeck coefficient and electrical conductivity of the 0.8 μm sample as a function of time, showing the trends as dedoping occured.

Figure 2(a) plots S versus σ for several pentacene average grain sizes that were determined by atomic force microscopy. For conduction by holes (which are the primary charge carriers in iodine-doped pentacene), S can be written as[13]

$$S = \frac{k}{q}\left(\frac{E_F - E_{tr}}{kT} - A\right), \tag{1}$$

where E_F, E_{tr}, k, and q are the Fermi energy, average carrier transport energy, Boltzmann constant, and unit charge, and A is a dimensionless parameter that accounts for asymmetric spread in the energy of conducting carriers near E_{tr}. For hopping transport that is characteristic of oligoacene crystals near room temperature,[14,15] the carrier density of states is usually modeled by a Gaussian distribution or symmetric exponential tails.[16–18] At low carrier concentrations, when E_F is several kT above E_{tr} (i.e., the Boltzmann limit), the energy-dependent electrical conductivity $\sigma(E)$ is approximately symmetric about E_{tr},[19] making A negligibly small. At high carrier concentrations, when E_F is near E_{tr}, carriers both above and below E_F contribute to transport, and A takes on a positive value, reducing S. Thus, in an experiment for which the dopant concentration drops over time, we expect the Seebeck coefficient to increase.

In the lightly-doped (Boltzmann) limit, the carrier concentration p can be written as

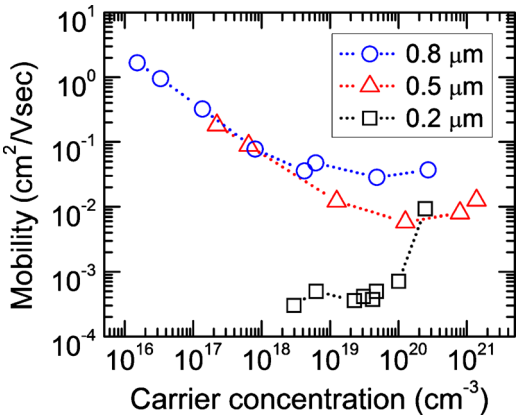

FIG. 3. (Color online) Carrier (hole) mobility derived from Eq. (3) as a function of carrier concentration for pentacene thin films with different grain sizes. Increasing mobility at lower carrier concentrations in 0.8 and 0.5 μm grain films is ascribed to a reduction in carrier-dopant scattering, while increasing mobility at higher carrier concentrations in the 0.2 μm grain film is ascribed to percolation effects in which transport between high-conductivity grains is enhanced as grain boundary carrier traps become filled.

$$p = P_0 \exp\left(-\frac{E_F - E_{tr}}{kT}\right) = P_0 \exp\left[-\frac{S}{(k/q)}\right], \quad (2)$$

where P_0 is the total hole density of states. The electrical conductivity $\sigma = pq\mu$ can then be substituted to yield

$$S = -\frac{k}{q}\ln\sigma + \frac{k}{q}(\ln\mu + \ln qP_0), \quad (3)$$

where μ is the hole mobility. The slope of $-k/q$ in S versus $\ln(\sigma)$ is illustrated by the dotted lines in Fig. 2(a). Because S does not fall below the $-k/q$ line for high conductivities, we assume that the Boltzmann approximation is valid and $A \approx 0$ for all samples shown. The y-intercepts are higher for larger grain sizes, which is consistent with their having higher intrinsic mobilities due to reduced grain boundary scattering.[20–22] For 0.5 and 0.8 μm grain sizes, there is a certain threshold conductivity near 10^{-2} S/cm, below which the Seebeck coefficient rises more rapidly than $-k/q$; we ascribe this to an increase in carrier mobility caused by a reduction in carrier-dopant scattering. This can also be seen in Fig. 2(b), which plots S and σ versus time for a series of measurements as dedoping occurs. Since we maintain a constant average sample temperature of 300 K, the decrease in carrier concentration is expected to be linear on a log-log plot of p versus t, dropping in proportion to $1/t^{\beta}$, where β is related to the order of the dedoping chemical reaction.[23] This dependence is consistent with the approximately linear increase measured for the Seebeck coefficient versus $\log(t)$, since $S \sim \ln(p)$ through Eq. (2). The conductivity (σ) drops at first in agreement with the drop in carrier concentration, but begins to approach a constant value, while the Seebeck coefficient continues to rise (i.e., the carrier concentration continues to fall). This is consistent with an increase in mobility.

The 0.2 μm grain size sample shows a different trend in which the deviation from $(-k/q)$ slope occurs for higher conductivities. We ascribe this to an increased mobility due to percolation-like transport between regions of high conductivity (i.e., the grains) that is enhanced as carrier traps at grain boundaries become filled. A similar result has been previously reported for vanadyl phthalocyanine thin films with similar grain size (50–200 nm) doped by a fluorinated form of tetracyano-quinodimethane.[10] Using Eq. (3) and setting P_0 to the molecular density of 2.9×10^{21} cm^{-3} (i.e., assuming one state per molecule[24]), we derive the mobility as a function of carrier concentration as shown in Fig. 3. The results are in general consistent with typical values of field-effect hole mobility measured for pentacene thin films with similar grain sizes.[21,25]

In summary, a low-noise measurement setup was used to characterize the dependence of thermoelectric transport parameters in polycrystalline pentacene thin films on doping and grain size. These measurements were then used to derive the bulk mobility, showing distinct transport regimes for larger and smaller grain sizes attributed to to the effects of carrier-dopant scattering and percolation, respectively.

This work was supported as part of the Center for Solar and Thermal Energy Conversion, an Energy Frontier Research Center funded by the U.S. Department of Energy, Office of Science, and Office of Basic Energy Sciences under Award No. DE-SC0000957.

[1]C. D. Dimitrakopoulos and P. R. L. Malenfant, Adv. Mater. (Weinheim, Ger.) **14**, 99 (2002).
[2]H. Klauk, M. Halik, U. Zschieschang, G. Schmid, W. Radik, and W. Weber, J. Appl. Phys. **92**, 5259 (2002).
[3]M. Gross, D. C. Müller, H.-G. Nothofer, U. Scherf, D. Neher, C. Bräuchle, and K. Meerholz, Nature (London) **405**, 661 (2000).
[4]S. E. Shaheen, C. J. Brabec, N. Serdar Sariciftci, F. Padinger, T. Fromherz, and J. C. Hummelen, Appl. Phys. Lett. **78**, 841 (2001).
[5]A. Shakouri and S. Li, Proceedings of the Eighteenth International Conference on Thermoelectrics, Baltimore, MD, 29 August-2 September 1999, (IEEE, Piscataway, NJ 1999), pp. 402–406.
[6]N. Mateeva, H. Niculescu, J. Schlenoff, and L. R. Testardi, J. Appl. Phys. **83**, 3111 (1998).
[7]D. Wang, L. Tang, M. Long, and Z. Shuai, J. Chem. Phys. **131**, 224704 (2009).
[8]A. von Mühlenen, N. Errien, M. Schaer, M.-N. Bussac, and L. Zuppiroli, Phys. Rev. B **75**, 115338 (2007).
[9]K. P. Pernstich, B. Rössner, and B. Batlogg, Nature Mater. **7**, 321 (2008).
[10]M. Pfeiffer, A. Beyer, T. Fritz, and K. Leo, Appl. Phys. Lett. **73**, 3202 (1998).
[11]B. Maennig, M. Pfeiffer, A. Nollau, X. Zhou, K. Leo, and P. Simon, Phys. Rev. B **64**, 195208 (2001).
[12]Y. Matsuo, S. Sasaki, and S. Ikehata, Phys. Lett. A **321**, 62 (2004).
[13]H. Fritzsche, Solid State Commun. **9**, 1813 (1971).
[14]V. Coropceanu, J. Cornil, D. A. da Silva Filho, Y. Olivier, R. Silbey, and J.-L. Brédas, Chem. Rev. (Washington, D.C.) **107**, 926 (2007).
[15]L. B. Schein, C. B. Duke, and A. R. McGhie, Phys. Rev. Lett. **40**, 197 (1978).
[16]O. Tal, Y. Rosenwaks, Y. Preezant, N. Tessler, C. K. Chan, and A. Kahn, Phys. Rev. Lett. **95**, 256405 (2005).
[17]R. Coehoorn, W. F. Pasveer, P. A. Bobbert, and M. A. J. Michels, Phys. Rev. B **72**, 155206 (2005).
[18]M. C. J. M. Vissenberg and M. Matters, Phys. Rev. B **57**, 12964 (1998).
[19]R. Schmechel, J. Appl. Phys. **93**, 4653 (2003).
[20]G. Horowitz and M. E. Hajlaoui, Adv. Mater. (Weinheim, Ger.) **12**, 1046 (2000).
[21]M. Shtein, J. Mapel, J. B. Benziger, and S. R. Forrest, Appl. Phys. Lett. **81**, 268 (2002).
[22]A. Di Carlo, F. Piacenza, A. Bolognesi, B. Stadlober, and H. Maresch, Appl. Phys. Lett. **86**, 263501 (2005).
[23]M. Brinkmann, V. S. Videva, A. Bieber, J. J. Andre, P. Turek, L. Zuppiroli, P. Bugnon, M. Schaer, F. Nuesch, and R. Humphry-Baker, J. Phys. Chem. A **108**, 8170 (2004).
[24]D. V. Lang, X. Chi, T. Siegrist, A. M. Sergent, and A. P. Ramirez, Phys. Rev. Lett. **93**, 086802 (2004).
[25]S. F. Nelson, Y.-Y. Lin, D. J. Gundlach, and T. N. Jackson, Appl. Phys. Lett. **72**, 1854 (1998).